

# A realistic approach to modeling an in-duct desulfurization process based on an experimental pilot plant study

F.J. Gutiérrez Ortiz\*, P. Ollero

*Departamento de Ingeniería Química y Ambiental, Universidad de Sevilla, Camino de los Descubrimientos, s/n, 41092 Sevilla, Spain*

Received 11 October 2007; received in revised form 10 January 2008; accepted 21 January 2008

## Abstract

This paper has been written to provide a realistic approach to modeling an in-duct desulfurization process and because of the disagreement between the results predicted by published kinetic models of the reaction between hydrated lime and SO<sub>2</sub> at low temperature and the experimental results obtained in pilot plants where this process takes place. Results were obtained from an experimental program carried out in a 3-MWe pilot plant. Additionally, five kinetic models, from the literature, of the reaction of sulfation of Ca(OH)<sub>2</sub> at low temperatures were assessed by simulation and indicate that the desulfurization efficiencies predicted by them are clearly lower than those experimentally obtained in our own pilot plant as well as others. Next, a general model was fitted by minimizing the difference between the calculated and the experimental results from the pilot plant, using Matlab™. The parameters were reduced as much as possible, to only two. Finally, after implementing this model in a simulation tool of the in-duct sorbent injection process, it was validated and it was shown to yield a realistic approach useful for both analyzing results and aiding in the design of an in-duct desulfurization process.

© 2008 Elsevier B.V. All rights reserved.

*Keywords:* Desulfurization; In-duct; SO<sub>2</sub>; Ca(OH)<sub>2</sub>; Kinetic; Model; Pilot plant

## 1. Introduction

The in-duct sorbent injection (DSI) desulfurization process is of great interest in regard to power plant retrofitting due to the small amount of capital required and the moderate operating costs involved. With regard to a desulfurization process using hydrated lime as the sorbent performed in conditions similar to those of DSI, a large disagreement between the experimental results obtained in pilot plant studies and those achieved in laboratory studies, from experiments carried out mostly in a fixed bed reactor, has been pointed out by several authors [1,2]. Thus, moderate desulfurization efficiencies of around 20–30%, and even higher, have been reached for a period of time of about 3 s or less in pilot plants [3,4]. However, under similar conditions to those used in pilot plants, the kinetic experiments carried out in a laboratory result in considerably lower removal of SO<sub>2</sub> and lime conversion for the same period of time.

The reaction of Ca(OH)<sub>2</sub> and SO<sub>2</sub> at low temperature was first studied by Klingspor et al. [5,6]. They used the shrinking core model to obtain the conversion of lime over time. They postulated that when the outer part of the sorbent particles is consumed, a more compact structure with a smaller surface area is exposed to the SO<sub>2</sub>. Thus, the decrease in the active area (related to the particle roughness) leads to a drastic drop in the reaction rate. Ruiz-Alsop and Rochelle [7] carried out kinetic studies in a fixed bed using inert sand where the sorbent particles were dispersed to determine the effect of some inorganic and organic salts on the SO<sub>2</sub> capture for spray-drying (SD) systems. These authors also utilized the unreacted core model, under the assumption that the reaction rate is controlled by both chemical reaction and diffusion. They concluded that the reaction order of SO<sub>2</sub> is zeroth for chemical reaction control and first for diffusion control. Irabien et al. [8] proposed a real-surface model based on the solid surface heterogeneity to describe the adsorption kinetics of SO<sub>2</sub>. In this model, the adsorption activation energy is a linear function of coverage. Khinast [2] studied the process from a kinetic point of view both in the laboratory and on a pilot plant scale, proposing a reaction mechanism where the kinetic equations change while the sorbent conversion is changing. The limit

\* Corresponding author. Tel.: +34 95 448 72 60/61/65/68; fax: +34 95 446 17 75.

E-mail addresses: [fjgo@esi.us.es](mailto:fjgo@esi.us.es) (F.J. Gutiérrez Ortiz), [ollero@esi.us.es](mailto:ollero@esi.us.es) (P. Ollero).

### Nomenclature

BET	specific superficial area measured by the BET technique ( $\text{m}^2/\text{g}$ )
$C_{p,g}^0$	average specific heat capacity for the gas measured under constant pressure ( $\text{J}/\text{mol K}$ )
$C_{\text{SO}_2}$	$\text{SO}_2$ molar concentration in the gas ( $\text{mol}/\text{m}^3$ )
$d_p$	lime particle diameter ( $\mu\text{m}$ )
$E_{\text{act}}$	activation energy ( $\text{J}/\text{mol}$ )
$E_{\text{SO}_2, \text{overall}}$	overall desulfurization efficiency (%)
$E_{\text{Duct}}$	desulfurization efficiency in the duct (%)
$E_{\text{ESP}}$	desulfurization efficiency in the ESP (%), measured as a fraction of the duct desulfurization
$L$	effective duct length (m)
MW	molecular weight ( $\text{g}/\text{mol}$ )
$\dot{n}_f$	molar flow rate of fresh lime ( $\text{mol}/\text{s}$ )
$\dot{n}_r$	molar flow rate of recirculated reactive solid ( $\text{mol}/\text{s}$ )
$N_i$	superficial molar flow rate for the species $i$ ( $\text{mol}/\text{m}^2 \text{ s}$ )
$-r$	reaction rate – consumption of $\text{Ca}(\text{OH})_2$ ( $-\text{mol Ca}(\text{OH})_2 \text{ converted}/\text{m}^3 \text{ of reactor s}$ )
$-r_{\text{SO}_2}$	reaction rate – consumption of $\text{SO}_2$ ( $-\text{mol SO}_2 \text{ converted}/\text{m}^3 \text{ of reactor s}$ )
$R'$	recirculation relation (RR) corrected for the sorbent ( $\text{kg of sorbent recirculated}/\text{kg fresh lime}$ )
$R_g$	universal constant for gases ( $8.314 \text{ J}/\text{mol K}$ )
RH	relative humidity in the flue gas (%)
RR	total solid recirculation ratio ( $\text{kg}/\text{kg}$ )
$T$	temperature (K)
$u_j$	velocity of the phase $j$ ( $\text{m}/\text{s}$ )
$w$	dimensionless axial coordinate in the duct (–)
$X$	$\text{Ca}(\text{OH})_2$ molar conversion ( $\text{mol}/\text{mol}$ )
$Y_i$	molar fraction of the substance $i$ in the gas ( $\text{mol}/\text{mol}$ )
$z$	axial coordinate of the duct (m)

### Greek letters

$\rho$	molar density ( $\text{mol}/\text{m}^3$ )
$\phi$	superficial area fraction uncovered by product (–)
$\Delta H_r^\circ(T)$	reaction heat at a pressure of 1 atm and at the temperature $T$ (reaction between $\text{Ca}(\text{OH})_2$ and $\text{SO}_2$ ) ( $\text{J}/\text{mol}$ )
$\varepsilon$	volumetric fraction related to the gas or solid phase ( $\text{m}^3/\text{m}^3$ )

### Subscripts

g, G	gas
lime	hydrated lime
s, S	reactive solid (sorbent partially converted plus reaction product)
w	dimensionless axial coordinate in the duct (it varies from 0 to 1)
r	recirculated (in both molar and mass fluxes)

stage is the chemical adsorption reaction or the product layer diffusion, depending on the conversion of the sorbent. Likewise, he believed that pore closure or the loss of reacting surface could be responsible for the rapid decline in the reaction rate. Krammer et al. [9] proposed that the conversion during the first stage of the reaction between  $\text{Ca}(\text{OH})_2$  and  $\text{SO}_2$  can be described by a certain equation for a kinetically controlled adsorption process. Also, they were able to define four regions with different prevailing reaction mechanisms, indicating that, in the end, the reaction rate drops significantly possibly because of pore closure. For Shih et al. [10] the surface coverage model was found to be the most suitable model to describe the reaction between  $\text{Ca}(\text{OH})_2$  and  $\text{CO}_2$ . Ho et al. [11] extended this conclusion to explain the reaction of  $\text{Ca}(\text{OH})_2$  sulfation. They suggested that the carbonation and sulfation of the hydrated lime are reactions controlled by chemical reaction on the surface of a grain, and the reacting surface area of the grain decreases with the deposition of solid product. Garea et al. [12] also studied the reaction between lime and  $\text{SO}_2$  by using neural networks. They confirmed that the results of the non-ideal adsorption kinetics in the mass balances of gas and solid phases provided a better prediction for lower values of dimensionless  $\text{SO}_2$  concentrations, which supposes higher  $\text{SO}_2$  removal efficiencies throughout the reactor. Bausach et al. [13] put forward a deactivation model and used an inverse shrinking core model with an ionic solid-state diffusion control, fitting it to experimental kinetic data. Their calculated values of the initial reaction rate in terms of  $dX/dt$  (sorbent conversion rate) are in the range of  $3.5 \times 10^{-4}$ – $1.7 \times 10^{-3} \text{ s}^{-1}$ , which corresponds to the range found experimentally by [5,6] ( $0$ – $2 \times 10^{-4} \text{ s}^{-1}$ , depending on the relative humidity, RH) and other researchers.

As can be seen, this kinetic modeling of the hydrated lime sulfation at low temperatures, in conditions similar to the DSI process, is quite complex and there is still not conclusive agreement. Furthermore, in this paper, different kinetic models have been adapted to the actual conditions of an in-duct desulfurization process, and the disagreement between predictions from these models and the experimental results obtained in a pilot plant, which are also published (i.e., [1,3]), is shown. Thus, a general kinetic model similar to the approaches of [9] and [10] has been adapted by minimizing the difference between the calculated and the experimental results from the pilot plant, using Matlab<sup>TM</sup>. The calculated values were obtained by simulation based on an in-duct desulfurization model together with a kinetic model. The final approach achieved is realistic for analyzing the process studied and assisting in its design, especially for engineers that operate in such plants. In any case, it should be clear that the results presented do not exactly correspond to a kinetic study.

## 2. Experimental set-up and data

The pilot plant (Fig. 1) is located within a power plant with a 550 MWe boiler that burns coal with a sulfur content of less than 0.7 wt%. There is a long gas duct upstream from a pilot precipitator to provide enough residence time for in-duct desulfurization.

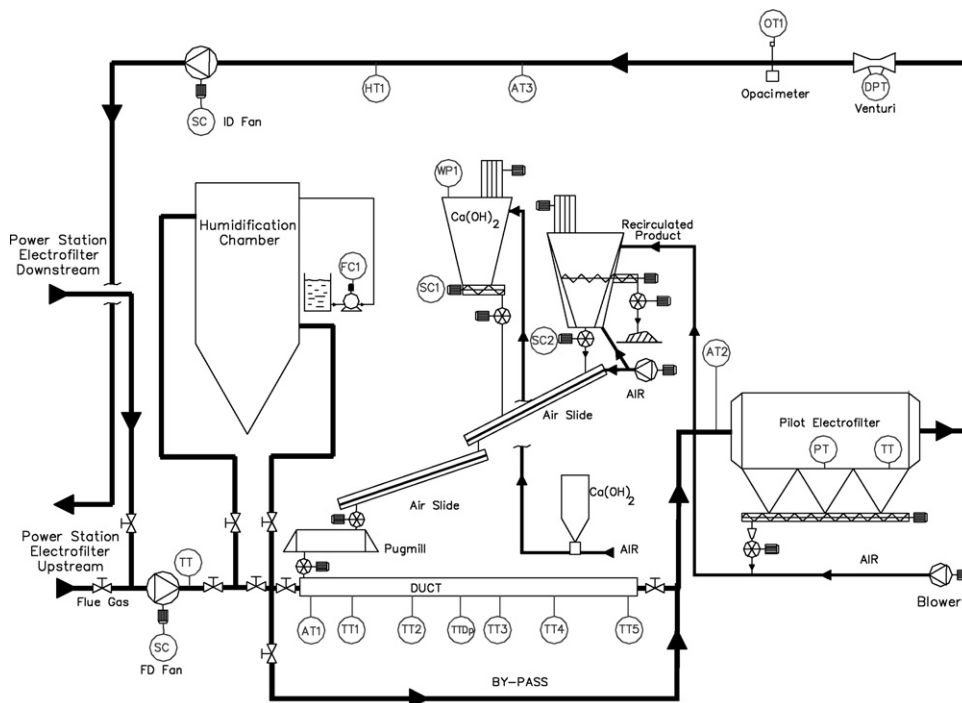


Fig. 1. Pilot plant flow sheet.

The duct is 50 m long and has an internal diameter of 0.44 m. This pilot plant can process up to 12,000 Nm<sup>3</sup>/h of flue gases that are drawn upstream and/or downstream from the power plant precipitator at 130–150 °C. Therefore, flue gas can or cannot have fly ash in any proportion, thus simulating the performance of an ash precollector located upstream from the desulfurization unit. There is also an SO<sub>2</sub> injection unit to increase the SO<sub>2</sub> gas concentration from 350 ppm to 3000 ppm. An SO<sub>2</sub> analyzer with three measuring probes – located at the pilot plant inlet, after the desulfurization unit and downstream from the electrostatic precipitator at the pilot plant outlet – makes it possible to determine the desulfurization efficiency in the duct and in the whole system, i.e., including the electrostatic precipitator (ESP).

At around 140 °C, the flue gas is sprayed with water to reduce its dry temperature to a few degrees above the adiabatic saturation temperature (about 51 °C), thus increasing its relative humidity. A mixture of fresh lime and recirculated product, which can be activated with liquid water in a pugmill, is injected downstream from the humidification chamber into the cooled, humidified flue gas. The SO<sub>2</sub> is removed in the duct and also in the ESP, which contributes significantly to the global yield (about 10% of the total) due to a long gas residence time (around 14 s) and the presence of unconverted lime. The dust collected in the ESP is conveyed to the product hopper by means of a pneumatic device. Both the fresh lime and product hoppers discharge through rotary valves into an air slide where both products are mixed. The air slide in turn discharges the mixture into the pugmill.

An experimental program was designed to evaluate the performance of the DSI process with respect to the main operating variables: the calcium-to-sulfur molar ratio (mol Ca/mol S), the

approach to the adiabatic saturation temperature (°C), the solid recirculation ratio (kg of recirculated solid/kg of fresh lime), the SO<sub>2</sub> flue gas concentration (ppm), the fly ash content in the flue gas (mg/Nm<sup>3</sup>), and the gas flow rate (Nm<sup>3</sup>/h). Table 1 shows the two levels considered for the five main variables used.

The experimental campaign included more than 40 tests to assess the effect of the different factors. These tests were used to obtain the realistic approach to modeling desired.

Commercial hydrated lime with a BET surface area of 12.9 m<sup>2</sup>/g, a mass average mean diameter of 6.83 μm, and a purity of 96 wt% was used. The fly ash had a mass average mean diameter of 12.20 μm, an unburnt amount of 3.02 wt% and a CaO content of 9.18 wt%.

This section is more specifically described elsewhere [14,15]. However, Figs. 2–4 summarize some of the experimental results that were important for attaining the realistic model. Fig. 2 shows the positive effects of increasing the fresh Ca/S ratio (CAS<sub>f</sub>) and of operating close to the adiabatic saturation temperature (AST). Fig. 3 indicates that the precollection of the fly ash has a clear positive effect on the desulfurization yield. Finally, Fig. 4 shows how a recirculation ratio (RR) of 10 can up to double the desulfurization yield obtained without sorbent recirculation.

Table 1  
Factors and levels in the experiences design used to obtain the model

Fresh calcium-to-sulfur ratio (mol/mol)	1.2–1.7
Approach to the adiabatic saturation temperature (°C)	8–13
SO <sub>2</sub> concentration (ppm)	350–1000
Gas flow rate (Nm <sup>3</sup> /h)	8000–12000
Ash concentration at the system inlet (mg/Nm <sup>3</sup> )	35–7000
Recirculation ratio (kg/kg)	0–10

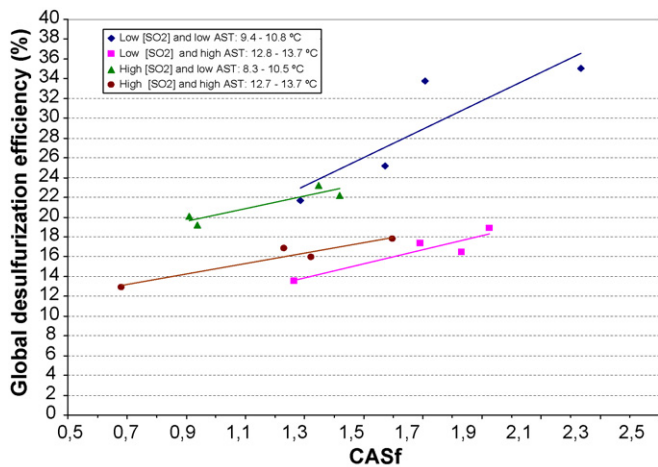


Fig. 2. Effect of the Ca/S ratio ( $CAS_f$ ) and the approach to the adiabatic saturation temperature (AST) on the global desulfurization efficiency.  $SO_2$  inlet concentrations vary from 350 ppm to 1000 ppm.

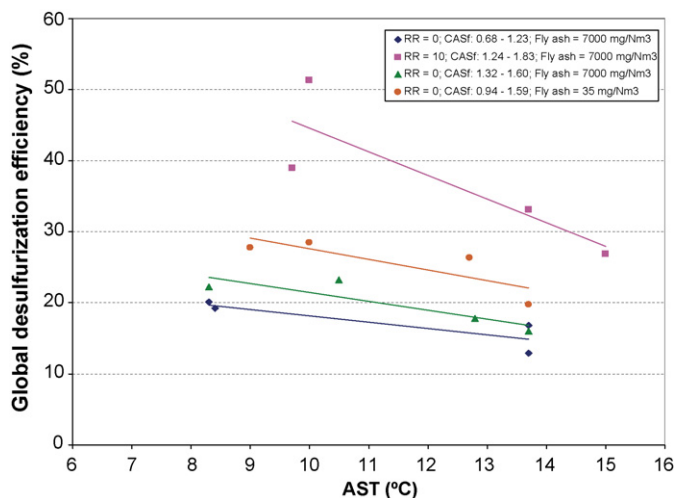


Fig. 4. Effect of the recirculation.

### 3. Modeling and simulation

#### 3.1. Previous kinetic models

In order to show the  $SO_2$  removal efficiencies for an induct desulfurization process using different kinetic models, five of them were selected: Klingspor et al. [5,6], Ruiz-Alsop and Rochelle [7], Irabien et al. [8], Khinast [2] and Krammer et al. [9]. Then, the units of the reaction rate were unified as follows:

$$\frac{\text{mol Ca(OH)}_2 \text{ converted}}{\text{m}^3 \text{ of reactor s}}$$

As a consequence of the disagreement found between the results obtained by the specific kinetic models cited above and the results obtained experimentally in the pilot plant, a general model was searched for, whose parameters could be fitted using the experimental results from the pilot plant. The basis for the

approach/model proposed, then, is the general model proposed by Shih et al. [10], which assumes that  $CO_2$  absorption (and, by extension, absorption of  $SO_2$ ) in  $Ca(OH)_2$  is controlled by the superficial reaction that takes place only in the reactive surface where there is no reaction product. In the general modeling, there is a parameter (“ $n$ ”) that can take different values linked to a function that represents how the reaction product covers the solid surface. These researchers chose  $n=1$  for the sake of simplicity, although the performance with a value of  $n=2$  would have been equally correct. In this latter case (logarithmic law), the following equation is yielded:

$$\frac{dX}{dt} = k_1 \exp(-k_2 X) \quad (1)$$

where  $X$  is the conversion of reactive solid.

Eq. (1) represents a model quite similar to those published by Irabien et al. [8] and Krammer et al. [9]. Indeed, Krammer et al. [9] used an equation similar to the one from the general model described by Shih et al. [10], as the exponent “ $n$ ” has a value of 2. Irabien et al. [8] suggested an exponential expression for the reaction rate as follows:  $r = k' \times \exp(-k'' \times \phi)$ , where  $\phi$  is the uncovered particle surface fraction. In this sense,  $k''$  may be approached as a deactivation rate constant, which is what Bausach et al. [13] called it.

#### 3.2. Modeling the desulfurization reaction

Shih et al. [10] studied the reaction between  $Ca(OH)_2$  and  $CO_2$ ; these authors extended the study afterwards to the reaction between  $Ca(OH)_2$  and  $SO_2$  [11], but they selected  $n=1$  without any explanation. The parameters  $k_1$  and  $k_2$  can depend on the BET surface area (BET), temperature ( $T$ ),  $SO_2$  concentration ( $C_{SO_2}$ ) and relative humidity (RH). Since these variables change through time while the process is running, it is not possible to achieve an analytical solution. To solve this obstacle, the effects for each parameter could be separated, as if they were the result of the product of a series of monovaryable

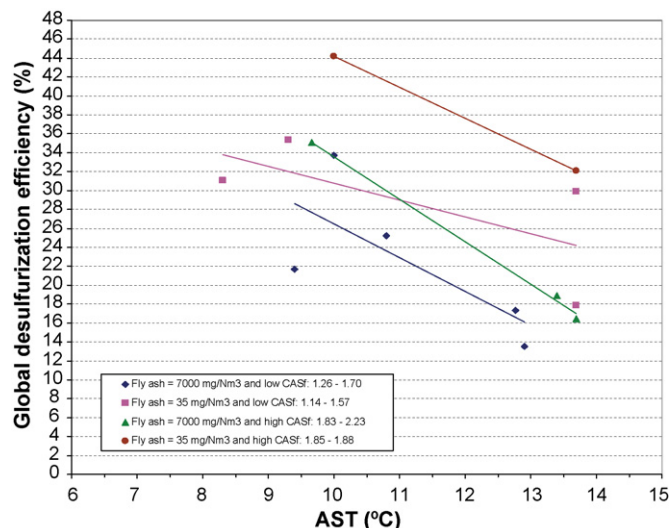


Fig. 3. Effect of the fly ash precollection.

functions, i.e.:

$$k_i = k_i^* f_{1i}(C_{\text{SO}_2}) f_{2i}(T) f_{3i}(\text{RH}) f_{4i}(\text{BET}) \quad i = 1, 2$$

$$k_i^* = \text{constant} \quad (2)$$

$$f_{1i}(C_{\text{SO}_2}) = k_{\text{SO}_2,i}^* C_{\text{SO}_2}^{m_i} \quad (3a)$$

$$f_{2i}(T) = k_{T,i}^* \exp\left(\frac{-E_{\text{act}}}{R_g T}\right) \quad (3b)$$

$$f_{3i}(\text{RH}) = k_{\text{HR},i}^* \exp\left(\frac{\text{RH}}{l_i}\right) \quad (3c)$$

$$f_{4i}(\text{BET}) = k_{\text{BET},i}^* \text{BET}^{t_i} \quad (3d)$$

where  $m_i$ ,  $l_i$  and  $t_i$  are constant coefficients.

Function  $f_{1i}$  assumes a  $m_i$ th-order kinetic with respect to the  $\text{SO}_2$  concentration; the function  $f_{2i}$  follows the Arrhenius law, and the function  $f_{3i}$  implies an exponential dependence of the kinetic parameter on the relative humidity. Finally, function  $f_{4i}$  suggests a proportional relationship to the  $t_i$ th power of the BET surface area. Most of these relationships have been already pointed out in most of the references cited in this paper.

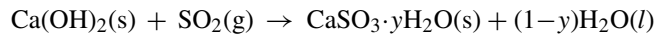
$k_2$  is related to the decrease in the conversion rate during the reaction, that is, while the conversion is increasing. Parameter  $k_1$  can be interpreted as the conversion rate when the conversion is very low (null, from a mathematical point of view). Beginning from the references cited above, where the kinetic models for the reaction of sulfation of  $\text{Ca}(\text{OH})_2$  have been chosen, and a previous study [15], the following considerations are established for the functions described above:

- The  $\text{SO}_2$  concentration could be linked to a kinetic of  $m_1$ th order (possibly the zeroth order), which affects parameter  $k_1$  in the equation of the conversion rate. If there is a function  $f_{12}$ , the exponent ( $m_2$ ) should be negative.
- Functions  $f_{21}$  and  $f_{22}$  can be lumped together with the constants associated with  $k_1$  and  $k_2$ , respectively, independent of the value of the corresponding activation energies, due to the narrow range of temperatures tested and used in a DSI process.
- For function  $f_{31}$ , coefficient  $l_1$  should be positive. However, for function  $f_{32}$ , coefficient  $l_2$  should be negative, and thus an increase in RH will be beneficial for the conversion rate.
- Taking into account the positive effect of the BET surface area in the adsorption models, exponent  $t_1$  should be positive, and  $t_2$  negative.

In the next section, the final kinetic equation is shown once fitted using the experimental results from the pilot plant.

### 3.3. Main equations of the in-duct model

#### 3.3.1. Considered reaction



being  $y < 1$ . Generally,  $y = 1, 1/2$ .

#### 3.3.2. Hypothesis

- There is a quasi-steady process.
- There is plug flow in all the phases (gas and solid).
- Conditions vary axially.
- Average values of density and flow rate for the gas phase are used.
- The loss of pressure along the duct is negligible.
- The particle diameter is the average value and it remains constant.
- The system is adiabatic, i.e., loss of heat to the exterior is insignificant.
- The hydrated lime is exclusively comprised of  $\text{Ca}(\text{OH})_2$ ,  $\text{CaCO}_3$  and  $\text{H}_2\text{O}$ .

$w = z/L$ , where  $z$  is the axial coordinate for the duct, and  $L$  is the duct length. That is,  $w$  is the dimensionless axial distance from the duct entrance (between 0 and 1).

#### 3.3.3. Equations

##### 3.3.3.1. Mass balance for the gas phase.

$$\frac{dN_{\text{SO}_2}}{dz} = \varepsilon_g \rho_g u_g \frac{dY_{\text{SO}_2}}{L dw} = -(-r_{\text{SO}_2})$$

$$= -r \left( \frac{\text{mol Ca}(\text{OH})_2 \text{ conv}}{\text{m}^3 \text{ reactor s}} \right) \quad (4)$$

where  $N_{\text{SO}_2}$  is the superficial molar flow rate for the  $\text{SO}_2$  ( $\text{mol}/\text{m}^2 \text{ s}$ ),  $\varepsilon_g$  is the volumetric fraction of the gas phase related to the duct ( $\text{m}^3/\text{m}^3$ ),  $\rho_g$  is the gas molar density ( $\text{mol}/\text{m}^3$ ),  $u_g$  is the velocity of the gas ( $\text{m}/\text{s}$ ),  $Y_{\text{SO}_2}$  is the molar fraction of the  $\text{SO}_2$  in the gas ( $\text{mol}/\text{mol}$ ) and  $(-r)$  is the reaction rate – consumption of  $\text{Ca}(\text{OH})_2$  – ( $\text{mol Ca}(\text{OH})_2$  converted/ $\text{m}^3$  reactor s)

##### 3.3.3.2. Mass balance for the solid phase.

$$\frac{dN_{\text{Ca}(\text{OH})_2}}{dz} = \varepsilon_s \rho_{\text{Ca}(\text{OH})_2} u_s \frac{d(1-X)}{L dw} = -(-r_{\text{SO}_2}) = -r \quad (5)$$

$$\varepsilon_s \rho_{\text{Ca}(\text{OH})_2} u_s \frac{dX}{L dw} = r \quad (6)$$

where  $N_{\text{Ca}(\text{OH})_2}$  is the superficial molar flow rate for the  $\text{Ca}(\text{OH})_2$  ( $\text{mol}/\text{m}^2 \text{ s}$ ),  $\varepsilon_s$  is the volumetric fraction of the reactive solid phase related to the duct ( $\text{m}^3/\text{m}^3$ ), and  $\rho_{\text{Ca}(\text{OH})_2}$  is the molar density of the lime ( $\text{mol}/\text{m}^3$ ).

##### 3.3.3.3. Energy balance.

$$\frac{dT}{L dw} = - \frac{r \Delta H_r^\circ(T)}{\varepsilon_g \rho_g u_g C_{p,g}^0(T)} \quad (7)$$

The molar concentration of SO<sub>2</sub> in the gas (mol/m<sup>3</sup>) – C<sub>SO<sub>2</sub></sub> – is calculated in these equations on wet basis. However, the C<sub>SO<sub>2</sub></sub> experimental data is expressed on dry basis.

From Eqs. (4) and (5), the following equation is derived:

$$Y_{\text{SO}_2, w} = Y_{\text{SO}_2, w=0} - \frac{\varepsilon_s \rho_{\text{Ca(OH)}_2}}{\varepsilon_g \rho_g} (X_w - X_{w=0}) \quad (8)$$

The boundary condition set for the sorbent conversion at the duct inlet implies an iterative process for solving the equation since it depends on the final conversion of Ca(OH)<sub>2</sub>, i.e.:

$$X_{w=0} = \frac{\dot{n}_r}{\dot{n}_f + \dot{n}_r} X_r = \frac{R' \text{MW}_{\text{lime}}}{\text{MW}_r + R' \text{MW}_{\text{lime}}} X_r \quad (9)$$

where  $\dot{n}_f$  is the molar flow rate of fresh lime (mol/s);  $\dot{n}_r$  is the molar flow rate of recirculated reactive solid (mol/s);  $R'$  is the recirculation relation (RR) corrected for the sorbent (kg of sorbent recirculated/kg fresh lime); MW is the molecular weight (g/mol)

Likewise, at the duct outlet:

$$X_r = X_{w=0} + \frac{Y_{\text{SO}_2, w=0} E_{\text{SO}_2, \text{overall}}(\%) }{100} \times \frac{\varepsilon_g \rho_g}{\varepsilon_{\text{lime}} \rho_{\text{Ca(OH)}_2}} \quad (10)$$

where:

$$\begin{aligned} E_{\text{SO}_2, \text{overall}}(\%) &= \frac{C_{\text{SO}_2, w=0} - C_{\text{SO}_2, w=1}}{C_{\text{SO}_2, w=0}} 100 \\ &\left( 1 + \frac{E_{\text{ESP}}(\%)}{100} \right) \\ &= E_{\text{Duct}}(\%) \left( 1 + \frac{E_{\text{ESP}}(\%)}{100} \right) \end{aligned} \quad (11)$$

and  $E_{\text{SO}_2, \text{overall}}$  is the overall desulfurization efficiency (%);  $E_{\text{Duct}}$  is the desulfurization efficiency in the duct (%);  $E_{\text{ESP}}$  is the desulfurization efficiency in the ESP (%), measured as a fraction of the duct desulfurization;  $E_{\text{ESP}}$  is an input data. The particle collector device was not modeled as part of the system. That is, the desulfurization removal and particle separation efficiencies in the ESP are data required by the simulator. However, to estimate these efficiencies, experimental results can be looked up [15], although most of them were about 10% of the total efficiency.

### 3.4. Simulation

Both the models obtained from the kinetic studies carried out at laboratory scale as well as the approach attained for modeling the desulfurization involved were simulated during the in-duct desulfurization process by means of a tool programmed in Visual Basic. This tool [14] has two main uses: first, it can be used to compare different kinetic models adapted to the configuration of a real plant for carrying out in-duct desulfurization, and, second, it can be used to assist in the design of a real plant once the suitable kinetic model is fitted. In this paper, the direct comparison between the kinetic models selected and the adapted general model, on the same scale and with equal operating conditions, is in view. In the simulation it is possible to run both the combustion

and humidification processes previous to the desulfurization, or only the latter process by setting the flue gas characteristics at the duct inlet. The integration process for the set of the ordinary differential equations of the model was performed using the classic 4th-order Runge–Kutta method. Besides the integration, it is necessary to carry out an iterative process as derived from the equations. As mentioned above, the boundary condition for the calculus of the sorbent conversion trend is given at  $z=0$ , i.e., at the duct inlet, and the expression of  $X$  at  $z=0$  includes the total conversion at the outlet of the particle collector device ( $X_r$ ).

## 4. Results and discussion

### 4.1. Fitting of the parameters

To fit the kinetic model described above from the experimental data, the following adaptation was performed:

$$(n = 2) \quad r = \frac{dX}{dt} \rho_{\text{Ca(OH)}_2} \varepsilon_s = k_1 \exp(-k_2 X) \rho_{\text{Ca(OH)}_2} \varepsilon_s \quad (12)$$

Taking into account the kinetic models selected, the general model and the proposed Eqs. (2), (3a), (3b), (3c) and (3d), and assuming that:

$$m_1 = 0; \quad m_2 = -1;$$

$f_{21}$  and  $f_{22}$  are embedded in the constants  $k_1$  and  $k_2$ ;

$$|l_1| \gg 1 \quad (l_1 > 0);$$

$$|l_2| \ll 1 \quad (l_2 < 0);$$

$$t_1 = 1; \quad t_2 = -1;$$

the following equation is reached:

$$\frac{dX}{dt} = K'_I \text{BET} \exp \left( - \frac{K'_{II} X}{(\text{RH}/100)(\text{BET}) Y_{\text{SO}_2}} \right) \quad (13)$$

This is very similar to what was postulated by Krammer et al. [9].

From the experimental results obtained in the pilot plant, it was possible to find out the values of the two parameters,  $K'_I$  and  $K'_{II}$ , by minimizing the quadratic deviation between the desulfurization efficiencies calculated using the model and those obtained experimentally. To achieve this, an in-duct model and the kinetic model were implemented in Matlab<sup>TM</sup> and an optimization algorithm with an objective function based on the Nelder–Mead algorithm, which represents the search for the minimum cited above, was used.

Since the parameters  $K'_I$  and  $K'_{II}$  were achieved by using a value of the BET surface area (12.9), the final model proposed was the following:

$$\frac{dX}{dt} = K_I \left( \frac{\text{BET}}{12.9} \right) \exp \left( - \frac{12.9 K_{II} X}{(\text{RH}/100)(\text{BET}) Y_{\text{SO}_2}} \right) \quad (14)$$

where the parameters  $K_I$  and  $K_{II}$  have the following values:

$$K_I = 0.0768; \quad K_{II} = 0.0019$$

The physical significance of these parameters is analogous to the corresponding ones from the general model ( $k_1$  and  $k_2$ ).

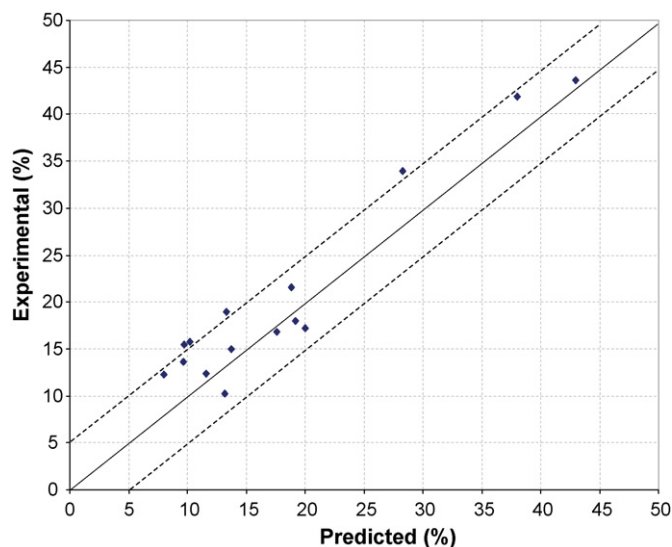


Fig. 5. Model validation: desulfurization efficiencies calculated and measured.

#### 4.2. Model assessment

As a model validation, some of the experimental tests were reserved to compare these results with those obtained by the model proposed. Fig. 5 shows the measured versus the calculated removal efficiencies for the duct. It can be seen that almost all the points lie in a narrow  $\pm 5\%$  band. Moreover, the standard deviation of the predicted values of dimensionless  $\text{SO}_2$  concentration related to the experimental ones was 0.032, with a correlation coefficient for data fitting of 0.957. As a further confirmation of the model proposed, an external study was used. Thus, recently, Garea et al. [12] published a paper where the data were obtained in an entrained flow reactor at laboratory scale (a reactor of 1 m length, 4 cm internal diameter). They used a commercial grade lime with an average particle diameter of 5.5  $\mu\text{m}$  and a BET surface area of 16  $\text{m}^2/\text{g}$ . Laboratory plant data covered the intervals of Ca/S ratio 1.5–18 (molar basis) and residence times 0.3–4 s. The unusually high molar ratio values of Ca/S in a real process

should be noted; unless a recirculation was considered as well as other details it is strange for the molar ratio to become so high in a real DSI process. They fitted two different models by using their data and a procedure based on neural networks. The first model (no. 1) was a grain modeling approach and the second model (no. 2) was a non-ideal adsorption modeling approach. The data available from this article were used to perform a simulation using the kinetic model adapted from the pilot plant tests in order to check how realistic the approach proposed is, as another way of validating it. Tables 2 and 3 sum up the results obtained by these authors (both experimental and fitted models) and by the proposed model using the simulation tool. Table 2 shows the results using three different Ca/S molar ratios ( $\text{CAS}_f$ ) and keeping the relative humidity (60%) and the temperature ( $60^\circ\text{C}$ ) constant. Table 3 illustrates the effect of the relative humidity on the desulfurization efficiency, with the  $\text{CAS}_f$  (4) and the temperature ( $60^\circ\text{C}$ ) constant. The  $\text{SO}_2$  concentration was always 1000 ppm at the reactor inlet, and the residence time for all cases was 2 s. It is clear that the proposed approach yields results similar to those presented by Garea et al. [12] and even better for some of the cases. Therefore, the modeling approach presented here can be considered quite realistic and useful for the analysis and design of a real in-duct desulfurization process.

#### 4.3. Comparative study of the kinetic models

In order to illustrate the main results obtained using different kinetic models, two practical cases were simulated. The input data are shown in Table 4.

A duct with dimensions similar to those of the one in the pilot plant was simulated. First the operation without solid recirculation was considered and then with recirculation (in italics in Table 4). Table 5 shows the main results obtained in the simulation.

Tables 6a and 6b illustrate the desulfurization efficiencies and the final conversion achieved for the two operation modes performed, i.e., with and without recirculation, at the duct outlet, for the different kinetic models considered. The fresh Ca/S

Table 2  
Simulation results with data from [12]; RH = 60%; temperature =  $60^\circ\text{C}$ ; residence time = 2s;  $\text{SO}_2$  inlet concentration = 1000 ppm

Ca/S ratio (molar basis), $\text{CAS}_f$	Desulfurization efficiency (%)			
	Experimental value	Model no. 1 [12]	Model no. 2 [12]	Proposed model
4	46	40	42	50.0
9	65	65	62	67.5
18	87	79	93	80.1

Table 3  
Simulation results with data from [12];  $\text{CAS}_f = 4$ ; temperature =  $60^\circ\text{C}$ ; residence time = 2s;  $\text{SO}_2$  inlet concentration = 1000 ppm

Relative humidity (%)	Desulfurization efficiency (%)			
	Experimental value	Model no. 1 [12]	Model no. 2 [12]	Proposed model
50	45	29	35	47.9
60	46	40	42	50.0
70	68	51	58	51.7

Table 4  
Input data for the simulation

Combustion process	
Coal (elemental composition) (wt%)	
Carbon	74.03
Hydrogen	4.14
Oxygen	6.54
Nitrogen	1.82
Sulfur	1.30
Humidity	2.45
Inert	9.72
Mass flow rate of coal (t/h)	1.2
Flue gas temperature at the desulfurization unit inlet (°C)	150
Pressure inside the boiler (bar)	1.013
Air	
Excess (%)	20
Relative humidity (%)	50
Inlet temperature (°C)	20
Humidification process	
Adiabatic saturation temperature approach (°C)	10
Fly ash removal efficiency (%)	100
Injected water temperature (°C)	20
Reaction process in the duct	
Commercial hydrated lime	
Ca(OH) <sub>2</sub> (wt%)	94
H <sub>2</sub> O (wt%)	1
CaCO <sub>3</sub> (wt%)	5
Density (kg/m <sup>3</sup> )	2350
Particle mean diameter (μm)	5
Specific area (BET) (m <sup>2</sup> /g)	12.9
Fly ash	
Density (kg/m <sup>3</sup> )	2600
Particle mean diameter (μm)	10
Operation	
Fresh calcium to sulfur molar ratio (Ca/S) (mol/mol)	2.0
Recirculation ratio (RR) (kg/kg)	0/10
Particles removal efficiency in the ESP (%)	98
Increment of the desulfurization efficiency in the ESP (%)	7
Design	
Duct length (m)	50
Duct inside diameter (m)	0.437
Tolerance	
For the conversion of Ca(OH) <sub>2</sub>	10 <sup>-7</sup>
For the conversion of SO <sub>2</sub>	10 <sup>-2</sup>

Table 5  
General results of the simulation

Combustion process	
SO <sub>2</sub> concentration (dry basis) (ppmv)	1029.38
SO <sub>2</sub> concentration (dry basis, 6% O <sub>2</sub> ) (ppmv)	885.77
SO <sub>2</sub> concentration (dry basis) (mg/Nm <sup>3</sup> )	2941.10
SO <sub>2</sub> in the flue gas (wet basis) (% vol)	0.10
CO <sub>2</sub> in the flue gas (wet basis) (% vol)	14.64
O <sub>2</sub> in the flue gas (wet basis) (% vol)	3.34
N <sub>2</sub> in the flue gas (wet basis) (% vol)	75.59
H <sub>2</sub> O in the flue gas (wet basis) (% vol)	6.33
Flue gas flow rate (wet) (Nm <sup>3</sup> /h)	11325
High heat value (dry) (kJ/kg)	30706
Low heat value (wet) (kJ/kg)	29716
Mass flow rate of fly ash (t/h)	0.090
Relative humidity in the flue gas (%)	1.37
Humidification process	
Mass flow rate of input water (t/h)	0.249
Mass flow rate of removed water and fly ash (t/h)	0.175
Mass flow rate of fly ash at the humidificator outlet (t/h)	0.000
Gas temperature at the humidificator outlet (°C)	60.68
Gas humidity at the humidificator outlet (%)	59.66
Gas flow rate (humid) (Nm <sup>3</sup> /h)	12046
Reaction process in the duct	
SO <sub>2</sub> concentration (dry basis), at the duct inlet (ppmv)	1029.4
Injected fresh lime flow rate (t/h)	0.08
Gas velocity (m/s)	27.29
Gas residence time (s)	1.832

Table 6a  
Simulation results with the selected kinetic models (RR = 0)

Kinetic model	Sorbent conversion inside the duct (%)	In-duct desulfurization efficiency (%)
Model of Ruiz-Alsop and Rochelle	0.397	0.793
Model of Klingspor et al.	0.008	0.015
Model of Irabien et al.	0.091	0.182
Model of Khinast	0.495	0.989
Model of Krammer et al.	0.425	0.850
Proposed model	10.980	21.970

removal efficiency and the sorbent conversion increased remarkably. It can be concluded that the real reaction rate should be about two orders of magnitude higher than values predicted by the kinetic studies carried out in laboratory. Only with the Khinast model is a desulfurization efficiency between those of the other four previous kinetic models and that of the realistic model

Table 6b  
Simulation results with the selected kinetic models (RR = 10)

Kinetic model	Sorbent conversion inside the duct (%)	In-duct desulfurization efficiency (%)
Model of Ruiz-Alsop and Rochelle	1.008	1.895
Model of Klingspor et al.	0.088	0.165
Model of Irabien et al.	0.897	1.687
Model of Khinast	5.582	10.500
Model of Krammer et al.	0.634	1.193
Proposed model	28.050	54.690

molar ratio was always 2. In Figs. 6 and 7 the trends of the SO<sub>2</sub> concentration along the duct are shown for the two operation modes simulated. Part of these figures is enlarged to show the evolution of the laboratory kinetic models that can be hardly distinguished from each other in the larger figure, due to the scale of the ordinate axis.

Against the predictions of the desulfurization efficiencies and the sorbent conversion by using the kinetic models chosen, which result in very low values, the model attained by the approach described in the previous section exhibits values that agree with those obtained in pilot plant studies. The residence time for the gas is about 2 s, quite a bit smaller than the duration of the tests carried out in the laboratory. Furthermore, when the recirculation is used, the values achieved for both the SO<sub>2</sub>



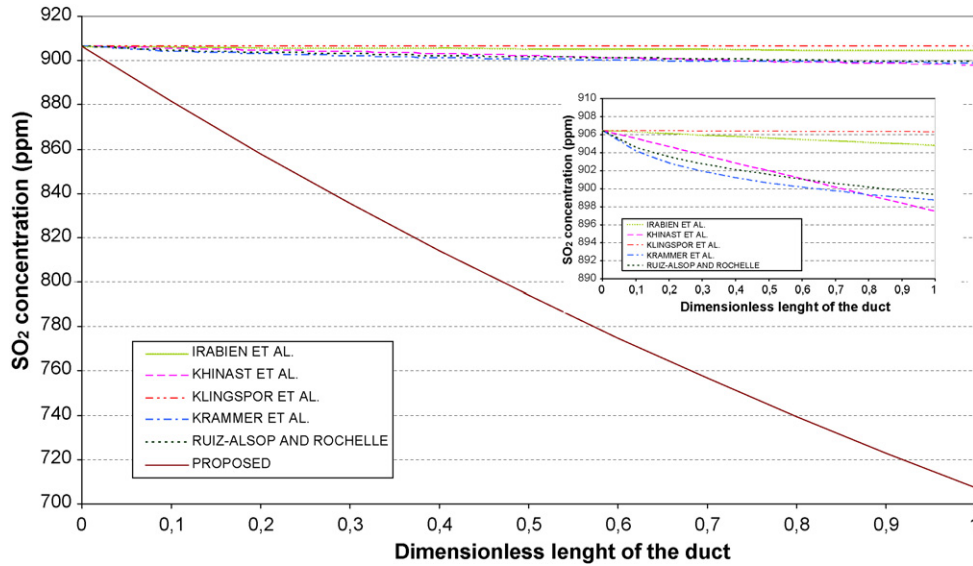


Fig. 6. Evolution of the SO<sub>2</sub> concentration (wet basis) throughout the duct (without recirculation).

obtained, although the values predicted by him are still far from the experimental values found in pilot plants.

Once the discrepancy is evident, it is inevitable to wonder why it occurs. Here are some possible explanations: first, it is noted that the kinetic models used were obtained at laboratory scale employing mostly fixed bed reactors; it seems to be more advisable to get a kinetic model with characteristics similar to those in an in-duct desulfurization process. This is directly related to the initial reaction rate (for the first seconds), which is surely quite a bit higher than that achieved after some minutes or even hours, in a fixed bed reactor. Second, it is possible that over the cool surface of lime particles (which enter the duct at ambient temperature or slightly higher), a transitory process of condensation of the gas humidity takes place. If this is the case, the SO<sub>2</sub> absorption and reaction mechanisms are different and considerably more effective than those when there are only a few layers of molecules of adsorbed water (2–3) because a gas–liquid reaction

is promoted instead of a gas–solid reaction. This phenomenon would obviously be transient since the lime particles would be heated downstream from the injection point and they would lose the water content progressively, by evaporation. However, in the pilot plant studies the reaction occurs for the most part in the first meters of the duct. Third, for the mode of operation with recirculation, it is possible that the covered surface of particles can be renewed frequently and efficiently, resulting in a higher exposure of the reactive surface. In this sense, the attrition of the particles in all the stages of the process must be considered, including the proper transport of sorbent along the duct, their separation in the ESP and subsequent pneumatic transport, their storage in a vibrated hopper and their final re-injection into the duct. Finally, this recirculated solid can pass through a pugmill where there could be a very efficient re-activation only with the partial humidification and/or a mixing of the solid prior to going in the duct. Of course, all of these hypotheses would require

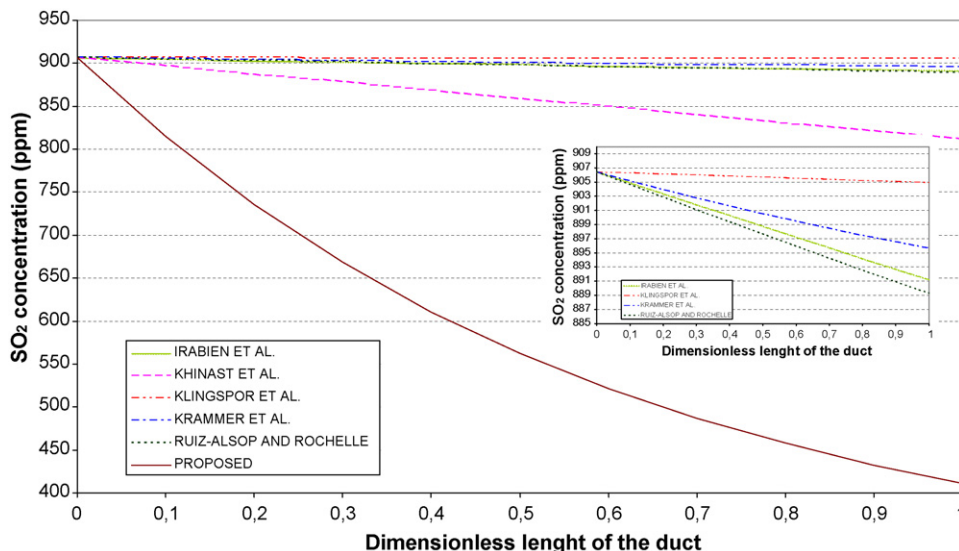


Fig. 7. Evolution of the SO<sub>2</sub> concentration (wet basis) throughout the duct (with recirculation).

further research to prove or disprove, which is clearly outside the scope of this article.

## 5. Conclusions

An extensive experimental program was performed in a 3-MWe pilot plant to assess the effects of the main operating variables. The experimental results are briefly summarized to support a realistic approach for modeling the desulfurization process involved. A general model was adapted from [10], which happens to be an approach similar to models by Irabien et al. [8] and Krammer et al. [9]. This model was fitted by minimizing the difference between the calculated and the experimental results from the pilot plant by means of simulation, using Matlab™. The parameters were reduced as much as possible (leaving only two), and finally the model was validated. Additionally, five kinetic models, from the literature, for the sulfation reaction of Ca(OH)<sub>2</sub> at low temperatures were assessed by simulation, and the desulfurization efficiencies predicted by them are clearly lower than those experimentally obtained in our own pilot plant as well as in others. However, the model adopted was shown to be a realistic approach, useful for both analyzing results and aiding in the design of an in-duct desulfurization process nearer to the industrial reality.

The divergence described above may have several causes. First, the reactor mainly used in the kinetic studies carried out is based on a fixed bed. Furthermore, the time of exposure should be very small. There may also be a condensation phenomenon over the lime particles in the first meters of the duct; finally, an attrition and renewal of the sorbent surface may occur, reactivating it after each pass through the system (in the case of the mode with solid recirculation).

## References

- [1] M.R. Stouffer, H. Yoon, F. Burke, An investigation of the mechanism of flue gas desulfurization by in-duct dry sorbent injection, *Ind. Eng. Chem. Res.* 28 (1989) 20–27.
- [2] J.G. Khinast, Kinetik Reaktionsmechanismus und Simulation eines Trockenen Rauchgasentschwefelungsverfahrens, Ph.D. dissertation, University of Graz, Austria, 1995.
- [3] M.R. Stouffer, W.A. Rosenhoover, J.A. Withum, Advanced cool-side desulfurization process, *Environ. Prog.* 12 (2) (1993) 133–139.
- [4] F.J. Gutiérrez Ortiz, P. Ollero, A pilot plant technical assessment of an advanced in-duct desulphurisation process, *J. Hazard. Mater.* B83 (2001) 197–218.
- [5] J. Klingspor, A.-M. Strömberg, H.T. Karlsson, I. Bjerle, A kinetic study of the dry SO<sub>2</sub> – limestone reaction at low temperature, *Chem. Eng. Commun.* 22 (1983) 81–103.
- [6] J. Klingspor, H.T. Karlsson, I. Bjerle, Similarities between lime and limestone wet-dry scrubbing, *Chem. Eng. Process.* 18 (1984) 239–247.
- [7] R. Ruiz-Alsop, G.T. Rochelle, Effect of relative humidity and additives on the reaction of sulfur dioxide with calcium hydroxide, Texas University at Austin, EPA, NTIS PB88-234174, Austin, Texas, 1988.
- [8] A. Irabien, F. Cortabitarte, M.I. Ortiz, Kinetics on flue gas desulfurization at low temperature: nonideal surface adsorption model, *Chem. Eng. Sci.* 47 (7) (1992) 1533–1543.
- [9] G. Krammer, Ch. Brunner, J. Khinast, G. Staudinger, Reaction of Ca(OH)<sub>2</sub> with SO<sub>2</sub> at low temperature, *Ind. Eng. Chem. Res.* 36 (1997) 1410–1418.
- [10] S.-M. Shih, C.-S. Ho, Y.-S. Song, J.-P. Lin, Kinetics of the reaction of Ca(OH)<sub>2</sub> with CO<sub>2</sub> at low temperatures, *Ind. Eng. Chem. Res.* 38 (1999) 1316–1322.
- [11] C.S. Ho, S.-M. Shih, C.-F. Liu, H.-M. Chu, C.-D. Lee, Kinetics of the sulfation of Ca(OH)<sub>2</sub> at low temperatures, *Ind. Eng. Chem. Res.* 41 (2002) 3357–3364.
- [12] A. Garea, J.A. Marques, A. Irabien, Modelling of in-duct desulfurization reactors, *Chem. Eng. J.* 107 (2005) 119–125.
- [13] M. Bausach, M. Pera-Titus, C. Fité, F. Cunill, J.-F. Izquierdo, J. Tejero, M. Iborra, Kinetic modeling of the reaction between hydrated lime and SO<sub>2</sub> at low temperature, *AIChE J.* 51 (5) (2005) 1455–1466.
- [14] F.J. Gutiérrez Ortiz, Estudio de Opciones de Mejora del Proceso de Desulfuración en Conducto de Gases de Combustión, Ph.D. dissertation, University of Seville, Spain, 2002.
- [15] F.J. Gutiérrez Ortiz, P. Ollero, Flue-Gas Desulfurization in an Advanced in-Duct Desulfurization Process: An Empirical Model from an Experimental Pilot-Plant Study, *Ind. Eng. Chem. Res.* 42 (2003) 6625–6637.